# Retrogression and Reaging Applied to Warm Forming of High-Strength Aluminum Alloy AA7075-T6 Sheet

THOMAS A. IVANOFF, JON T. CARTER, LOUIS G. HECTOR Jr., and ERIC M. TALEFF

This study introduces retrogression forming, a new warm-forming methodology for high-strength aluminum alloys such as AA7075-T6. Retrogression forming combines a retrogression heat treatment with simultaneous warm forming at approximately 200 °C to improve upon the room-temperature ductility of AA7075-T6, approximately 10 pct in tension, and can then use the automotive paint-bake cycle to restore nearly peak-aged strength. Experimental data indicate that retrogression forming at 200 °C provides a tensile ductility of 20 pct, approximately double that of room temperature, and that subsequent reaging by a simulated paint bake restores hardness to within 10 pct of the original peak-aged (T6) hardness. To explore the retrogression-forming concept, the retrogression behaviors of two AA7075-T6 sheet materials from different suppliers are characterized between 200 °C and 350 °C. The times and temperatures of retrogression treatments suitable for simultaneous warm forming are determined, and tensile ductilities under these conditions are measured. Tensile ductilities during high-temperature deformation (up to 520 °C) are measured and compared to those possible under retrogression-forming conditions. Plastic flow at temperatures of 460 °C to 520 °C is governed by dislocation-climb-controlled creep, a mechanism different from the behaviors observed under retrogression-forming conditions.

https://doi.org/10.1007/s11661-018-5084-3


## I. INTRODUCTION

MASS reduction[1–7] is of paramount importance in transportation industries, the automotive industry in particular, as a means to improve the fuel economy and general performance of future vehicles, including those using alternative powertrain technologies. One approach to mass reduction is increasing the use of materials with greater strength-to-weight ratios than conventional materials currently used in the automobile body-in-white. Medium-strength aluminum alloys, such as AA6111 and AA5182, were previously used to achieve mass reductions. For example, an all-aluminum cradle saved 10 kg over a steel cradle in the 1999 Chevy Impala,[8] and aluminum body panels saved 175 kg over steel panels in aluminum-intensive Mercury Sable vehicles.[9] Additionally, hot forming has been studied as a means to improve formability of medium-strength Al-Mg-Si alloys.[10,11] High-strength aluminum alloy sheet materials potentially can reduce mass in critical vehicle components, such as side-impact beams, pillars, and rails,[12,13] by replacing components formed from steel or lower-strength aluminum alloys.[14] Aluminum alloy 7075 (AA7075) is of interest [13] because it exhibits high strength in the peak-aged condition, 505 MPa yield strength, and 570 MPa tensile strength minimums in the T6 temper,[15] and its density is one-third that of steel. However, AA7075-T6 exhibits poor formability in stamping at room temperature because its ductility is limited to approximately 10 pct tensile elongation. Consequently, AA7075-T6 has not seen extensive use in the complex component shapes currently required by vehicle bodies.

Elevated temperatures can significantly improve the tensile ductility of AA7075-T6,[16–19] though the microstructural changes responsible for this improvement are not well understood. Elongations-to-failure as high as 25 pct at 230 °C[16,17] and more than 50 pct at 460 °C[18] have been reported for AA7075. For additional context, the tensile ductilities observed for AA7075 and

THOMAS A. IVANOFF is with the Sandia National Laboratories, Materials Mechanics & Tribology, P.O. Box 5800, Mail Stop 0889, Albuquerque, NM 87185. Contact e-mail: tivanof@sandia.gov JON T. CARTER and LOUIS G. HECTOR, Jr. are with General Motors, Research and Development, MC 480-106-RL1, 30470 Harley Earl Blvd., Warren, MI 48092-2031. ERIC M. TALEFF is with the Department of Mechanical Engineering, The University of Texas at Austin, Austin, TX 78712.

Manuscript submitted 15 September, 2018.
Article published online January 1, 2019

**Table I. Tensile Elongations of Sheet Materials Relevant to the Transportation Industry at Several Temperatures and Strain Rates**

| Material | Temperature (°C) | Elongation (Pct) | Strain Rate ($s^{-1}$) | References | Notes |
|---|---|---|---|---|---|
| AA5182 | 300 | 51 | $1 \times 10^{-1}$ | 20 | a |
| | 400 | 137 | $1 \times 10^{-2}$ | 20 | a |
| AA5083 | 300 | 100 | $1 \times 10^{-1}$ | 21 | b |
| | 400 | 200 | $1 \times 10^{-1}$ | 21 | b |
| | 450 | 200 | $1 \times 10^{-1}$ | 21 | b |
| | 500 | 150 | $1 \times 10^{-1}$ | 21 | b |
| AA6061-T6 | 21 | 17 | | 19,22 | |
| AA6061-T4 | 21 | 25 | | 19 | |
| AA6016-T4 | 21 | 28 | | 23,24 | |
| AA6111-T4 | 21 | 28 | | 24 | |
| | 350 | 23 | $1 \times 10^{-2}$ | 20 | a |
| | 450 | 85 | $1 \times 10^{-2}$ | 20 | a |
| AA7075-O | 21 | 17 | | 19 | |
| | 340 | 45 | $1 \times 10^{-2}$ | 18 | b |
| | 460 | 60 | $1 \times 10^{-2}$ | 18 | b |
| AA7075-T6 | 21 | 11 | | 19 | |
| | 220 | 18 | $7.8 \times 10^{-2}$ | 16 | a |
| | 260 | 16 | $7.8 \times 10^{-2}$ | 16 | a |
| DP Steel Alloys | 21 | 15 to 30 | | 25 | c |
| HSLA Steel Alloys | 21 | 10 to 25 | | 26,27 | d |

[a]Initial strain rate is reported.
[b]It is not stated whether initial strain rate or true-strain rate is reported.
[c]Data are reported for DP steels containing ferrite and 10 to 30 pct martensite with Si or P alloying additions. Uniform tensile elongation is reported.
[d]Data are reported for HSLA steel grades SAE 950X and 980X and for HSLA steels VAN 80, VAN 50, and VAN QN by Jones and Laughlin Steel Corp. Uniform tensile elongation is reported.

other commercially available aluminum alloys are listed in Table I at various temperatures. Also included for comparison are the tensile ductilities of some dual-phase (DP) and high-strength-low-alloy (HSLA) steels at room temperature. The elevated-temperature ductility of AA7075-T6 significantly exceeds the approximately 10 pct tensile elongation reported at room temperature.[19] However, subsequent heat treatments are typically required to restore the T6 temper after forming at elevated temperatures (ex. 460 °C), and those can be complex and expensive. Elevated-temperature forming might be much more useful to manufacturing practice if a method to quickly and easily restore a high strength similar to the T6 condition after forming is developed. It is of note that the improved ductility at approximately 200 °C has been used to warm form side-impact beams in AA7075 for a performance car,[12] but without using the aspects of retrogression forming described herein to recover hardness lost during warm forming.

The high strength of the AA7075-T6 alloy is attributed to numerous fine $\eta'$ and fewer $\eta$ ($MgZn_2$) intermetallic precipitates distributed throughout the aluminum matrix.[28] These are plate-like with diameters from 3 to 10 nm and 5 to 17 nm, respectively.[28] Annealing above 130 °C will considerably decrease yield strength and hardness of the alloy by reducing the number of fine $\eta'$ and $\eta$ precipitates.[28] Because of this, it is difficult to maintain peak-aged strength in AA7075-T6 sheet material after forming or annealing at temperatures greater than 130 °C. This is particularly challenging for vehicle manufacturing, which requires a paint-bake cycle. The paint-bake cycle can involve one or a series of baking steps, wherein each step cures a different coat of paint applied to the body-in-white. One example of a paint-bake cycle to cure three successive coats of paint is as follows: bake from (1) 160 °C to 185 °C for 20 to 30 minutes, (2) 125 °C to 150 °C for 20 to 30 minutes, and (3) 115 °C to 135 °C for 20 to 30 minutes.[29] Any forming process for AA7075-T6 conducted at elevated temperature must be designed in concert with the paint-bake cycle to achieve a strength preferably equivalent to the peak-aged condition. Ideally, such a forming process will not require any post-forming heat treatments other than paint baking. Results from previous experiments suggest a potential for the paint-bake cycle to function as a reaging treatment following retrogression, although only a portion of the strength lost during retrogression might be recovered.[16,37] Therefore, a warm-forming technology that utilizes only the paint-bake cycle to restore AA7075 to near peak-aged strength is of interest from a scientific standpoint and for the potential to lower forming complexity and cost.

A process that is particularly intriguing for AA7075-T6 forming is retrogression and reaging (RRA).[30] RRA is a two-step heat treatment. First, a retrogression heat treatment is applied. That is followed by, second, a reaging heat treatment. Retrogression is a heat treatment that can be applied to peak-aged, precipitation-strengthened aluminum alloys, including AA7075-T6.[30] Retrogression may be performed over a range of temperatures and times, but the retrogression temperature must be greater than the aging temperature and less than the solutionizing temperature of the material. The aging and solutionizing temperatures for

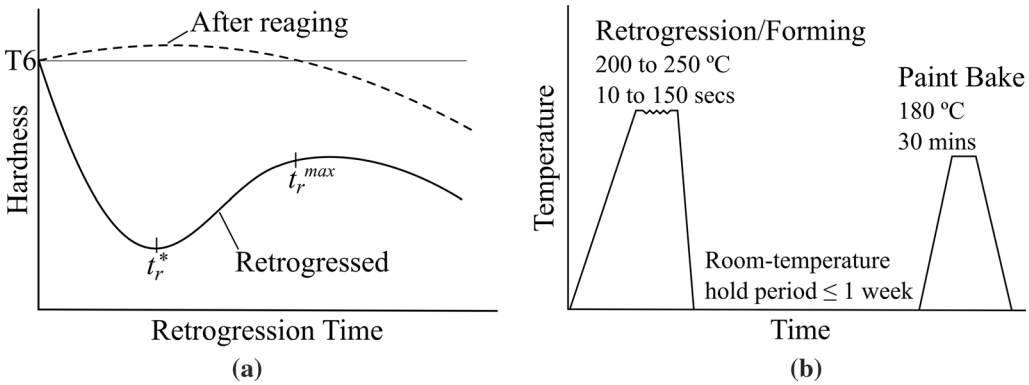


Fig. 1—(*a*) The response of an AA7075-T6 material to a standard RRA heat treatment. Hardness is displayed as a function of retrogression time from the peak-aged condition after retrogression (solid curve) and after subsequent reaging (dashed curve). Note the optimal retrogression time, $t_r^*$, and the limit for the recovery of peak-aged hardness by reaging, $t_r^{max}$, shown for this retrogression temperature. (*b*) The processing temperature history of a hypothetical retrogression-forming process for AA7075-T6.

AA7075 are 120 °C and 460 °C, respectively.[19] Data from Cina and Park demonstrate that AA7075-T6 can be retrogressed under conditions that range from 30 minutes at 180 °C to 60 seconds at 240 °C.[30,31] The typical material response to a retrogression heat treatment is illustrated by the solid curve shown in Figure 1(a), which presents a schematic of hardness as a function of retrogression time at a single retrogression temperature. Hardness initially decreases with time to a local minimum, recovers slightly, and then monotonically decreases. It is typical to retrogress material to the time $t_r^*$, noted in Figure 1(a), which denotes the location of the local minimum in hardness during retrogression. The minimum denotes a desirable retrogressed condition because peak-aged hardness lost during retrogression can be fully recovered during subsequent reaging. Note that peak-aged hardness cannot be fully recovered if the material is retrogressed beyond the time $t_r^{max}$, noted in Figure 1(a).[30,33] Reaging of AA7075 after retrogression is typically performed for 24 hours at 120 °C, the standard age-hardening temperature for this alloy.[19] The dashed line in Figure 1(a) depicts the material response after reaging following retrogression. The dissolution of fine (5 to 10 nm) $\eta'$ and $\eta$ intermetallic precipitates during retrogression and their reformation during reaging, as described in the extant literature,[31–36] governs RRA behavior.

The literature demonstrates through transmission electron microscopy (TEM) and selected area electron diffraction (SAED) that during retrogression the concentrations of the hardening precipitates, fine (5 to 10 nm) $\eta'$ and $\eta$, are reduced by (1) dissolution of fine $\eta'$ precipitates; (2) transformation of larger $\eta'$ precipitates into $\eta$ precipitates; and (3) coarsening of prior $\eta$ precipitates to $> 20$ nm, especially those present along grain boundaries.[31–36] During reaging, the concentration of $\eta'$ precipitates increases by the regrowth of partially dissolved $\eta'$ and the formation of new $\eta'$.[34] The $\eta$ precipitates already present may coarsen. The resulting RRA material contains a number of fine $\eta'$ and $\eta$ precipitates nearly equal to that of the peak-aged (T6) material.[34] Thus, the strength of the RRA material recovers to peak-aged values after the RRA treatment. The most common use of RRA treatments for AA7075 is to improve resistance to stress corrosion cracking,[30–36] which is a result of the changes to precipitate structures at grain boundaries, particularly the formation of coarse ($> 20$ nm) $\eta$ precipitates at the expense of fine $\eta'$ and $\eta$ precipitates.

Unlike the existing studies of AA7075-T6 heat treatment behavior, the present study presents elements of a new methodology, termed retrogression forming, that combines retrogression heat treatments with warm forming near 200 °C and an industrially relevant paint-bake cycle to recover near peak-aged strength with no additional heat treatments. Retrogression is conducted concurrently with warm forming to increase ductility. The paint-bake cycle is used as a reaging step to recover hardness lost during the concurrent warm forming and retrogression. Figure 1(b) illustrates the processing temperature history of a hypothetical retrogression-forming process for AA7075-T6. This study pursues the experimental data necessary to describe the key changes in mechanical properties governed by precipitate evolution during RRA, the relationship of these changes to diffusion processes, and the practical potential of the retrogression-forming methodology. The tensile ductility of AA7075-T6 at temperatures and times compatible with concurrent retrogression is quantified. The material response to retrogression, which here means hardness variation with time, is evaluated. The subsequent recovery of hardness, a surrogate for tensile strength,[42] by reaging through a simulated paint-bake cycle applied after retrogression is also quantified. Tensile ductility is reported from uniaxial tensile tests at room temperature (21 °C), a warm-forming temperature (200 °C), and hot-forming temperatures (300 °C to 520 °C). The tensile deformation behaviors within these different temperature regimes are explored and compared. The data reported are used to identify conditions that are compatible with improving ductility in AA7075-T6 through warm forming and subsequently restoring nearly peak-aged strength through a simulated paint bake. It is concluded that retrogression can be produced during warm forming at 200 °C while approximately doubling ductility

and that reaging to within 10 pct of the peak-aged strength is possible through a simulated paint bake applied to AA7075-T6.

## II. MATERIALS AND EXPERIMENTAL METHODS

### A. *Materials*

Two AA7075-T6 sheet materials, referred to herein as materials A and B, were obtained from two different suppliers in the peak-aged condition. Both materials had an as-received sheet thickness of 2 mm. Elemental compositions were determined using X-ray fluorescence (XRF) analysis with a Horiba XGT-7200™ X-ray analytical microscope, and are shown in Table II together with specification limits of the AA7075 alloy.[38,39] Elemental compositions were determined after calibrating with a pure copper reference because an AA7075 reference standard was not available. This may explain why some elemental compositions for materials A and B appear outside of the designated composition limits for AA7075. The relative differences in elemental composition between the materials are less likely to be affected. Compared to material B, material A has lower concentrations of Zn, Mg, Cu, and Si, and therefore might be expected to exhibit a lower peak-aged hardness.

Specimens were prepared for polarized light optical microscopy by mechanical grinding, polishing, and then electrolytic etching (20 V) with Barker's reagent (1.8 pct fluoboric acid in 98.2 pct distilled water)[40] to produce color contrast between grains when viewed under polarized light. Figure 2 presents the microstructures of materials A and B in both the as-received T6 and the solutionized conditions. The solutionizing treatment involved annealing at 480 °C for 2 hours, followed by water quenching. Grain sizes were measured along the short-transverse direction (STD) and the rolling direction (RD) in the as-received and the solutionized conditions using the lineal-intercept method described in ASTM E112.[41] Average grain sizes are provided with standard deviations of the measurements in Table III. Both materials exhibit the elongated grain structures expected of rolled sheet material, as demonstrated in Figure 2. Grain size after solutionizing changed little for

**Table II. The Specified Chemical Composition Limits of AA7075 and the Measured Compositions of Materials A and B, in Weight Percent**

| Elements | Zn | Mg | Cu | Cr | Fe | Si | Mn | Ti | Al |
|---|---|---|---|---|---|---|---|---|---|
| Spec.[38] | 5.1 to 6.1 | 2.1 to 2.9 | 1.2 to 2.0 | 0.18 to 0.28 | < 0.5 | < 0.4 | < 0.3 | < 0.2 | Bal. |
| Material A | 6.12 | 1.74 | 1.76 | 0.17 | 0.27 | 0.0 | 0.03 | 0.04 | Bal. |
| Material B | 6.29 | 2.34 | 1.91 | 0.21 | 0.14 | 0.33 | 0.01 | 0.04 | Bal. |

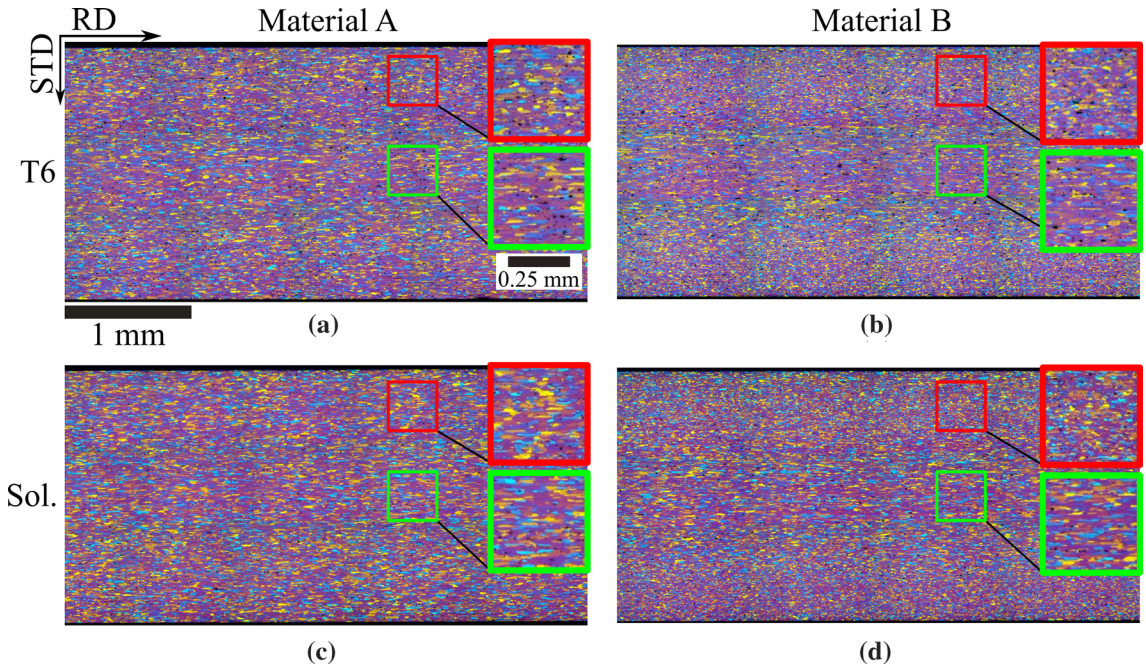


Fig. 2—Microstructures for material A in the (*a*) peak-aged (T6) and (*c*) solutionized (Sol.) conditions and material B in the (*b*) peak-aged and (*d*) solutionized conditions. Grain sizes measured along the rolling direction (RD) and the short-transverse direction (STD) are provided in Table III.

either material, as demonstrated in Table III; also compare Figures 2(a) and (b) and compare Figures 2(c) and (d). Some difference between grain sizes at the sheet surface and sheet center is noted for each material, with finer grains near the surface, and this difference is most pronounced in material B.

### B. *Heat Treatment Experiments*

Heat treatment experiments were conducted on rectangular specimens with dimensions of 2 × 10 × 30 mm, excised from materials A and B in the as-received T6 condition. These specimens were used to evaluate the effects of several different heat treatments involving retrogression. Retrogression treatments were performed in a molten salt bath at temperatures of 200 °C, 225 °C, 250 °C, 300 °C, and 350 °C for times ranging from 10 to 150 seconds. The salt bath controlled specimen temperature to within approximately ± 3 °C of that desired. Following retrogression, specimens were held at room temperature (approximately 21 °C) for 1 week prior to reaging. This hold period was implemented to reflect conditions where formed components are typically trimmed, cleaned, and applied to a vehicle body-in-white over the course of several days before paint baking. Specimens were then either retained in the retrogressed condition or subjected to further heat treatment in a resistance tube furnace to evaluate reaging. The tube furnace controlled temperature to within approximately ± 3 °C of that desired. Three heat treatments were used to study reaging behavior. The first employed the typical reaging treatment of 120 °C for 24 hours.[19] The second was a simulated paint-bake treatment of 180 °C for 30 minutes, which reflects one industry practice for paint baking.[29] The third employed the standard reaging treatment followed by the simulated paint-bake treatment. Specimens were thus produced in the following four conditions: retrogressed only (R); retrogressed and reaged (RA); retrogressed and paint baked (RP); or retrogressed, reaged, and paint baked (RAP). These four heat treatments are summarized in Table IV with the labels used to reference each. The results of these experiments were used to determine the retrogression conditions from which peak-aged strength can be recovered during subsequent reaging.

At each heat-treating step, temperature was monitored with one or more K-type thermocouples. Specimens were quenched to room temperature (approximately 21 °C) in water immediately following each heat treatment. The final quenching step was applied for consistency among experiments but is unlikely to be needed in the practical application of retrogression forming. The material response to heat treatment was measured using Vickers hardness tests (HV10) at room temperature; hardness can be used as a reasonable surrogate for tensile strength in aluminum alloys.[42] Hardness tests were conducted using a load of 10 kg and a load hold time of 15 seconds. Each hardness value reported is an average of three to five individual measurements, and error bars used in the figures represent an average of the standard deviations across all hardness measurements. Specimens in all heat-treated conditions were stored at room temperature (approximately 21 °C), and hardness tests were intermittently performed over a period of three years to measure the effects of natural aging. These tests were conducted because AA7075 is susceptible to natural aging at room temperature in some temper conditions.[19,37]

**Table III. Lineal-Intercept Grain Sizes Measured Along the Rolling Direction (RD) and Short-Transverse Direction (STD) from Just Below the Sheet Surface and at the Center of Materials A and B in the Peak-Aged and Solutionized Conditions**

| | Center (μm) | | Surface (μm) | |
|---|---|---|---|---|
| | STD | RD | STD | RD |
| Peak-Aged (T6) | | | | |
| Material A | 13 ± 9 | 58 ± 42 | 15 ± 10 | 44 ± 33 |
| Material B | 14 ± 10 | 49 ± 34 | 11 ± 6 | 28 ± 19 |
| Solutionized | | | | |
| Material A | 13 ± 9 | 41 ± 27 | 14 ± 9 | 47 ± 28 |
| Material B | 13 ± 8 | 43 ± 29 | 11 ± 7 | 26 ± 15 |

### C. *Uniaxial Tensile Tests*

Tensile tests were conducted at room and elevated temperatures using computer-controlled electromechanical and servo-hydraulic mechanical testing machines. Tests were performed in displacement control mode with a computer adjusting displacement rate based on cross-head or piston motion to maintain an approximately constant true-strain rate during testing. Rates for

**Table IV. Material Heat Treatment Conditions, Their Abbreviations, and the Retrogression Temperatures and Times for Each Heat Treatment Condition**

| Material Condition | Label | Retrogression Temperatures (°C) | Retrogression Times (s) |
|---|---|---|---|
| Retrogressed Only | R | 200, 225, 250, 300, and 350 | 10, 30, 90, and 150 |
| Retrogressed and Then Reaged with the Simulated Paint Bake (180 °C for 30 min) | RP | 200, 225, and 250 | 10, 30, 90, and 150 |
| Retrogressed and then Reaged at 120 °C for 24 h | RA | 200 and 225 | 10, 30, 90, and 150 |
| Retrogressed, Aged at 120 °C for 24 h, and Then Reaged with the Simulated Paint Bake (180 °C for 30 min) | RAP | 200 and 225 | 10, 30, 90, and 150 |

Specimens were water quenched after retrogression heat treatment and after reaging heat treatment.

this control were calculated assuming uniform specimen deformation and constant specimen volume. Strain is reported from an extensometer for room-temperature tests and from piston motion for elevated-temperature tests; an elevated-temperature extensometer was not available for this study. Room-temperature (approximately 21 °C) tests were conducted with the electromechanical testing machine. Elevated-temperature (200 °C and greater) tests were conducted with the servo-hydraulic mechanical testing machine; specimen temperature during these tests was controlled using a furnace coupled to the mechanical testing machine. Two different furnaces were used, one for testing at low temperature (200 °C) and the other for testing at high temperatures (≥ 300 °C). Dog bone-shaped tensile specimens were designed according to ASTM standards E8, E21, and E2448.[43–45] Specimens were water-jet cut from the as-received materials. Different specimen geometries were required by the furnace and gripping fixture combinations available for tensile testing at different temperatures and are described in Table V. The rolling direction was oriented either parallel or perpendicular to the tensile direction and is noted for each individual test result presented. All tensile specimens retained the as-received sheet thickness of 2 mm for materials A and B prior to testing.

Tensile tests were conducted at 200 °C in order to evaluate ductility under warm-forming conditions. A convective box furnace maintained this test temperature during testing. It was determined from the heat treatment experiments that exposure to the testing temperature at 200 °C should not exceed 150 seconds to guarantee the recovery of peak-aged strength during subsequent reaging. Specimen exposure time to this testing temperature was limited by using the following rapid-heating technique. Specimens were first preheated to 110 °C in less than 20 minutes in a resistance tube furnace. Data available in the literature demonstrate that the microstructure of AA7075-T6 is not significantly altered by annealing at temperatures below 120 °C for this short time.[19] This was confirmed by experiments that measured hardness before and after such low-temperature soaks. Specimens were then placed between two copper plates held at the desired test temperature, 200 °C, within the convective box furnace for 60 seconds to reach the testing temperature. Specimens were then transferred to tensile grips in the convective furnace within approximately 30 seconds. Tensile testing began within a maximum of 60 seconds and was completed within an additional 20 seconds. Tested specimens were then extracted and quenched to room temperature (approximately 21 °C) in water within 20 to 40 seconds. The longest time from specimen insertion into the furnace at 200 °C through specimen quenching is 210 seconds. Because the time to reach 200 °C, estimated as 60 seconds, is included in this time, the experiments met the goal of limiting total specimen time at temperature to approximately 150 seconds. Specimen temperature during testing was controlled to within ± 3 °C of the desired test temperature. The temperature of the specimen was monitored during testing using two K-type thermocouples in contact with the surface of the specimen. Specimens were tested in tension at approximately constant true-strain rates of $1 \times 10^{-1}$, $5 \times 10^{-2}$, and $1 \times 10^{-2}$ $s^{-1}$.

Tensile tests at 300 °C, 460 °C, 480 °C, 500 °C, and 520 °C were conducted to evaluate ductility under hot-forming conditions, for which partial or full solutionization of AA7075 is expected.[19] Tensile specimens were solutionized at 480 °C for 2 hours immediately prior to testing to prevent the precipitate dissolution process from influencing deformation behavior. Test temperature was controlled using a split-tube three-zone resistance furnace. The furnace was preheated to the desired temperature prior to testing. The specimen was then transferred to the furnace and brought to the desired temperature; temperature during testing was controlled to within ± 3 °C. The temperature of the specimen was monitored during testing with two K-type thermocouples in contact with the surface of the specimen. Tests were conducted at approximately constant true-strain rates from $3 \times 10^{-4}$ to $3 \times 10^{-1}$ $s^{-1}$. Specimens were immediately quenched to room temperature (approximately 21 °C) in water upon the completion of tensile deformation.

## III. RESULTS

### A. *Retrogression*

Vickers hardness measurements after retrogressing at 200 °C, 225 °C, 250 °C, 300 °C, and 350 °C are presented in Figure 3(a) for material A and Figure 3(b) for

**Table V. The Tensile Specimen Geometries Used for Room-Temperature, Warm-Temperature, and Hot-Temperature Uniaxial Tensile Tests**

| | | | Specimen Dimensions (mm) | | | | |
|---|---|---|---|---|---|---|---|
| Category | Furnace | Temp. (°C) | Grip Length | Grip Width | Gage Length | Gage Width | Transition Radius |
| Room Temperature | N/A | 21 | 25.4 | 12.7 | 75 | 6 | 3.2 |
| Warm Temperature | convective box | 200 | 25 | 25 | 25 | 6 | 1.5 |
| Hot Temperature | three-zone split tube | 300 | 25.4 | 12.7 | 75 | 6 | 3.2 |
| | | 460 to 520 | 25.4 | 12.7 | 25.4 | 6 | 3.2 |

material B as functions of retrogression time. The retrogression behaviors in Figure 3 can be grouped into two categories based upon the potential to recover hardness to peak-aged values through reaging. Either the hardness lost during retrogression is recoverable to nearly peak-aged values upon reaging or the hardness lost during retrogression cannot be recovered. Retrogression treatments conducted at 200 °C, 225 °C, and 250 °C demonstrate a local minimum in hardness, as shown in the schematic of Figure 1(a). Note that the local minimum in hardness at 200 °C is not readily determined from Figure 3 and might occur at retrogression times greater than those considered in this study. Within the vicinity of this local hardness minimum, there is a potential to fully recover hardness through subsequent reaging. The extant literature suggests that after retrogression of AA7075-T6 material at these temperatures and times, peak-aged hardness and strength can be recovered through an appropriate reaging treatment.[30–33] As retrogression temperature increases from 200 °C to 250 °C, the severity of the initial reduction in hardness increases, and the time required to reach the local minimum hardness value, $t_r^*$, decreases. For both materials A and B, $t_r^*$ occurred at 10, 30, and 150 seconds or longer for retrogression at 250 °C, 225 °C, and 200 °C, respectively. The reduction in hardness at $t_r^*$ increased from 12 to 20 pct for material A and from 9 to 15 pct for material B as retrogression temperature increased from 200 °C to 250 °C. It is noted from Figure 3 that material A typically exhibits a 3 to 5 pct greater reduction in hardness from retrogression than does material B for a given retrogression temperature and time. The reason for this discrepancy is not explored here, but potential causes are later discussed. The absence of local hardness minima in Figure 3 at 300 °C and 350 °C demonstrates that the hardness decreases in both materials A and B are unrecoverable after retrogression at these temperatures. Although shorter retrogression times might allow some hardness recovery during reaging, such short times are not of practical importance to retrogression forming. For this reason, retrogression at temperatures of 300 °C and higher is not further considered.

To better represent and understand the combined effects of temperature and time on hardness reduction during retrogression heat treatments, a method for constructing a single-master curve from hardness data is proposed. This method uses the Arrhenius relationship[46] to combine time and temperature into a temperature-compensated retrogression time, $\tau$, against which hardness can be plotted to produce a single curve among data from the different retrogression temperatures investigated. This technique assumes that the dissolution of precipitates during retrogression depends primarily on a single diffusion process, likely either Zn or Mg in Al, governed by a single activation energy. The temperature-compensated retrogression time is defined as

$$\tau = t \cdot e^{-Q/RT_R}, \qquad [1]$$

where $Q$ is the activation energy for dissolution of $\eta'$ and $\eta$ precipitates (J/mol); $R$ is the universal gas constant (J/mol-K); $T_R$ is the retrogression temperature (K); and $t$ is the retrogression time (s). The value for $Q$ is taken as 95 kJ/mol, based upon data reported by Balderach *et al.* for precipitate dissolution in Al-Zn-Mg alloys, obtained using differential scanning calorimetry.[37]

Vickers hardness after retrogression at temperatures from 200 °C to 350 °C is presented in Figure 4 as a function of the temperature-compensated retrogression time, $\tau$, for materials A and B. Hardness data from Park[31] and from Kanno *et al.*[32] at the local hardness minimum, *i.e.*, $t_r^*$ in Figure 1(a), are included for comparison. All data from materials A and B fall reasonably well onto the single dashed curve drawn in Figure 4. The most important feature of Figure 4 is that a single value of temperature-compensated retrogression time, $\tau_r^*$, describes the location of the local hardness minimum for all these data, including data from the literature, across a range of retrogression temperatures. The bracket shown above the $\tau_r^*$ label in Figure 4 indicates the approximate uncertainty in the local

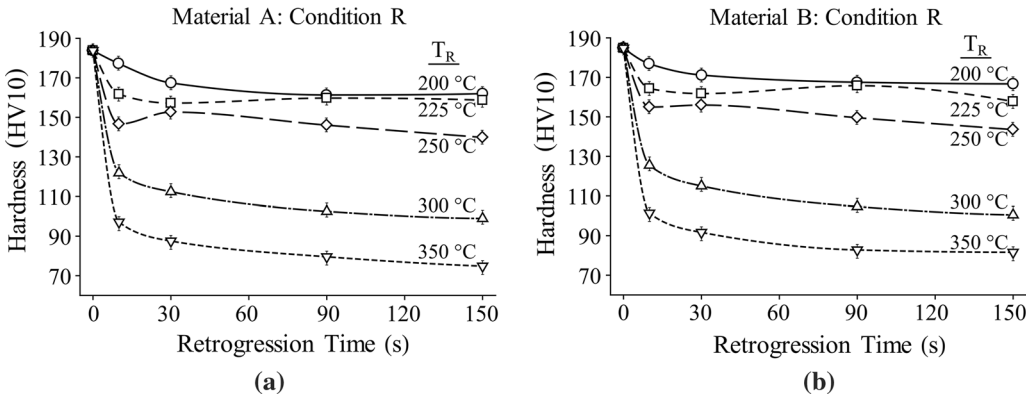


Fig. 3—Vickers hardness (HV10) measurements after retrogression at temperatures ($T_R$) of 200 °C, 225 °C, 250 °C, 300 °C, and 350 °C are presented as functions of retrogression time for (*a*) material A and (*b*) material B. The time required to reach the local minimum in hardness is defined as $t_r^*$. For both materials A and B, $t_r^*$ occurred at 10, 30, and 150 s or longer for retrogression at 250 °C, 225 °C, and 200 °C. No local hardness minimums are observed after retrogression at 300 °C and 350 °C.

hardness minimum for the data presented. The average value for $\tau_r^*$ in Figure 4 is $3.6\times10^{-9}$ seconds, and its minimum and maximum values are $2.3\times10^{-9}$ and $5.4\times10^{-9}$ seconds, respectively. Note that this value for the temperature-compensated retrogression time can be used with Eq. [1] to describe the retrogression time necessary to reach the local hardness minimum for any given retrogression temperature. For example, the $t_r^*$ value for retrogression at 200 °C is predicted as 110 seconds with minimum and maximum values of 70 and 165 seconds, respectively, using Figure 4. For both materials A and B, Figure 3 demonstrates for retrogression at 200 °C that $t_r^*$ occurred at 150 seconds, which falls within the predicted range of values for $t_r^*$ using Figure 4. The hardness values at $\tau_r^*$ vary between 135 and 181 HV10 with material and with retrogression temperature, as might be expected. Note that in Figure 3, for example, the local minimum hardness value is different at each retrogression temperature. Despite the differences in the local hardness minimum between the materials and retrogression temperatures, the local minimum reliably occurs at a consistent value of temperature-compensated retrogression time, $\tau_r^*$, of approximately $3.6 \times 10^{-9}$ seconds, and this provides a useful means of predicting optimal retrogression treatments across a range of retrogression times and temperatures.

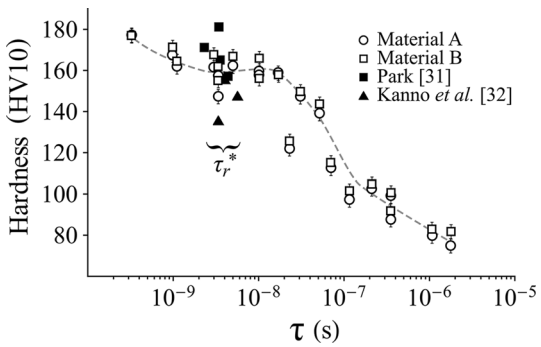


Fig. 4—Vickers hardness (HV10) measurements on materials A and B are presented as a function of temperature-compensated retrogression time, τ. Local minimum hardness values from retrogressed AA7075-T6 materials documented in the literature are presented for comparison.[31,32] Note that the optimal temperature-compensated retrogression time, $\tau_r^*$, is indicated and is approximately $3.6 \times 10^{-9}$ s.

## B. *Reaging*

The viability of recovering hardness through a simulated paint bake after retrogression was investigated. Specimens were naturally aged for one week following retrogression, prior to application of a simulated paint-bake treatment of 180 °C for 30 minutes. Reaging experiments were conducted with the simulated paint bake on specimens retrogressed at 200 °C, 225 °C, and 250 °C. Figure 5 presents Vickers hardness measurements after paint-bake reaging, which demonstrates that peak-aged hardness was not fully recovered in either material A or B. Hardness, however, did increase by 3 to 10 pct from the retrogressed condition for specimens of material A that were retrogressed at 200 °C and 225 °C and for specimens of material B that were retrogressed at 200 °C. The hardnesses of these specimens after paint-bake reaging were within 5 to 10 pct of the peak-aged (T6) condition. Material B retrogressed at 225 °C did not display any appreciable recovery of hardness through reaging with the simulated paint bake. Both materials retrogressed at 250 °C recovered significant hardness through the simulated paint bake compared to their retrogressed conditions, but the final hardnesses never approached peak-aged values. Retrogression treatments conducted at 250 °C were not investigated further because hardness was not sufficiently recovered at this temperature to make it of interest.

The hardnesses of materials A and B after retrogression and reaging with the simulated paint bake are compared with hardness values produced by other reaging procedures shown in Figure 6. Vickers hardness measurements from the following conditions are presented as a function of retrogression time for retrogression temperatures of 200 °C and 225 °C: retrogressed only (R); retrogressed and paint baked (RP); retrogressed and reaged (RA); and retrogressed, reaged, and

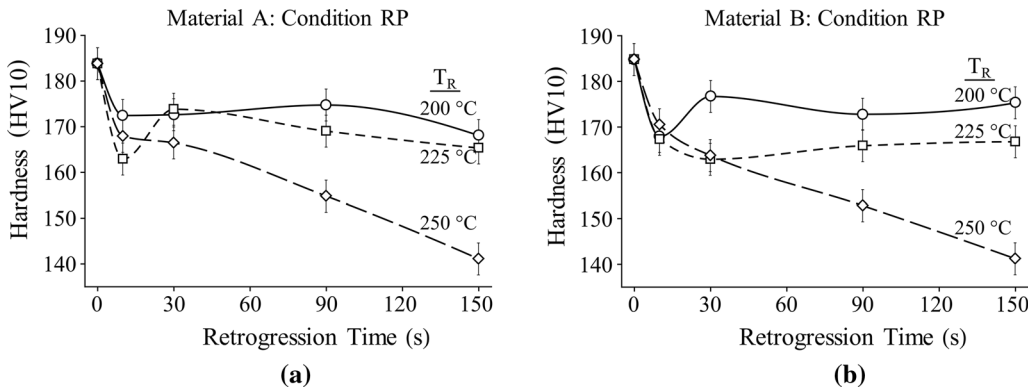


Fig. 5—Vickers hardness (HV10) measurements are presented after retrogression at temperatures ($T_R$) of 200 °C, 225 °C, and 250 °C, natural aging at 21 °C for 1 week, and a simulated paint bake at 180 °C for 30 min; hardness is plotted as a function of retrogression time for (*a*) material A and (*b*) material B.

then paint baked (RAP). The effectiveness of a reaging procedure can be evaluated by comparing the hardness produced to the peak-aged (T6) hardness and to the hardness after retrogression.

Figure 6(a) presents the hardness of material A after retrogression at 200 °C (curve R) and the three different reaging procedures investigated in this study (curves RA, RP, and RAP). Note that T6 hardness, measured from material A in the as-received, peak-aged condition, is marked in Figure 6(a). Curve RA demonstrates that the standard reaging procedure increases hardness by 10 to 20 pct from the retrogressed condition (curve R) and recovers the full T6 hardness of material A. Curve RP illustrates that hardness in material A increased by 3 to 10 pct from the retrogressed condition after reaging with the simulated paint bake, with the exception of the specimen retrogressed for only 10 seconds. Hardness remains between 5 and 10 pct below peak-aged hardness for the RP specimens. The RAP reaging procedure produced hardness increases from the retrogressed condition that are similar to those produced by the RP reaging procedure, as demonstrated by Figure 6(a). Figure 6(b) presents the hardness of material B after retrogression at 200 °C and after subsequent reaging. T6 hardness is marked in Figure 6(b) as measured from material B in the as-received, peak-aged condition. The standard reaging procedure, curve RA, recovered hardness to within 3 pct of the peak-aged value, with the exception of the specimen retrogressed for 150 seconds at 200 °C. The paint-bake reaging, curve RP, increased hardness by 5 to 8 pct over the retrogressed condition for retrogression times of greater than 10 seconds. However, the hardnesses of the RP specimen remained approximately 5 to 10 pct less than the peak-aged (T6) condition. The RAP procedure did not increase hardness significantly over the retrogressed condition.

Figure 6(c) presents the hardness of material A after retrogression at 225 °C and after subsequent reaging. The standard reaging procedure recovered hardness in material A to nearly peak-aged values after retrogression at 225 °C for 10 and 30 seconds, but not for 90 and 150 seconds, as illustrated by curve RA in Figure 6(c). The RP and RAP procedures generally increased hardness by 5 to 12 pct over the retrogressed condition in material A after retrogression at 225 °C. Figure 6(d) presents the hardness of material B after retrogression at 225 °C and after reaging. Similar to material A after retrogression at 225 °C, Figure 6(d) demonstrates that the standard reaging procedure, curve RA, recovered hardness to nearly peak-aged values for retrogression times of 10 and 30 seconds, but not for 90 and 150 seconds in material B. The RP and RAP procedures

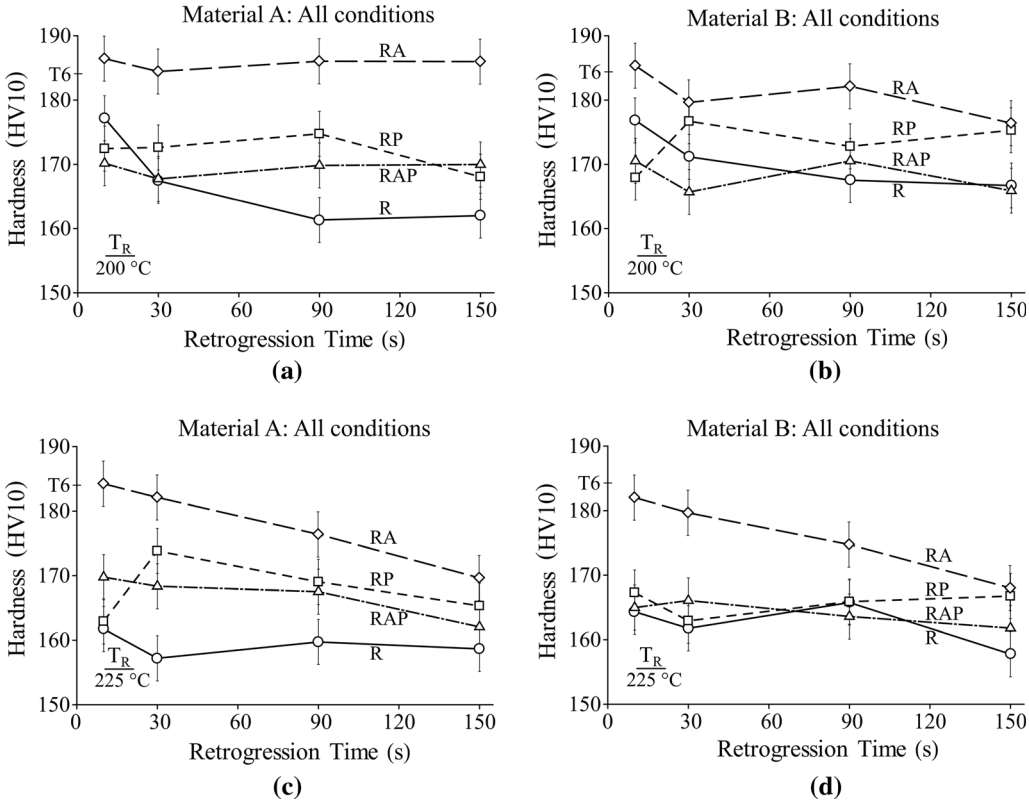


Fig. 6—Vickers hardness (HV10) measurements of material A retrogressed at (*a*) 200 °C and (*c*) 225 °C and material B retrogressed at (*b*) 200 °C and (*d*) 225 °C are presented as functions of retrogression time for multiple heat treatment conditions. The material condition abbreviations R, RA, RP, and RAP are described in Table IV. Initial hardnesses in the as-received T6 condition, measured as 183.8 HV10 for material A and 184.8 HV10 for material B, are noted.

did not improve hardness in material B over the retrogressed conditions, as demonstrated in Figure 6(d).

### C. *Natural Aging*

The effect of natural aging on the hardness of materials A and B after retrogression at 200 °C and subsequent reaging with the simulated paint-bake cycle was monitored for over three years. Vickers hardness measurements are shown as a function of the logarithm of natural aging time for four different retrogression times in Figure 7. The hardnesses of materials A and B in the retrogressed condition, shown in Figures 7(a) and (b), respectively, changed with natural aging time. There is a slight increase in hardness over time, most pronounced in the materials retrogressed for 10 seconds. Figures 7(c) and (d) present the hardnesses of materials A and B, respectively, after retrogression at 200 °C and reaging with a simulated paint bake at 180 °C for 30 minutes. Natural aging did not significantly affect either material in the retrogressed and paint-baked (RP) condition. The natural aging of materials A and B retrogressed at 225 °C was also monitored. Because results from the materials retrogressed at 225 °C mimic the materials retrogressed at 200 °C, those data are not presented. The hardnesses of the materials retrogressed at 225 °C also increased with natural aging time, but the RP condition is similarly stable to the RP materials retrogressed at 200 °C.

### D. *Tensile Tests*

Uniaxial tensile tests at 200 °C were conducted to examine the tensile ductilities possible from AA7075-T6 under deformation conditions suitable for retrogression from which peak-aged strength can be recovered during subsequent reaging (see Figure 6(a) for material A and Figure 6(b) for material B). Deformation behavior was examined at 200 °C because the retrogression time to the local minimum in hardness, $t_r^*$, occurred at 150 seconds or longer for retrogression at 200 °C in both materials studied (see Figure 3), which maximizes the time available for retrogression-forming operations compared to the other retrogression temperatures investigated. Additionally, deforming at the lowest retrogression temperature studied, 200 °C, suggests less energy expenditure without sacrificing significant gains in ductility compared to higher temperatures. Tests were conducted at approximately constant true-strain rates of $1 \times 10^{-1}$, $5 \times 10^{-2}$, and $1 \times 10^{-2}$ $s^{-1}$. Rapid-heating procedures, described in the materials and experimental methods section, limited the specimen's time at 200 °C to a maximum of approximately 150 seconds, which is within the time $t_r^*$ indicated by the data shown in

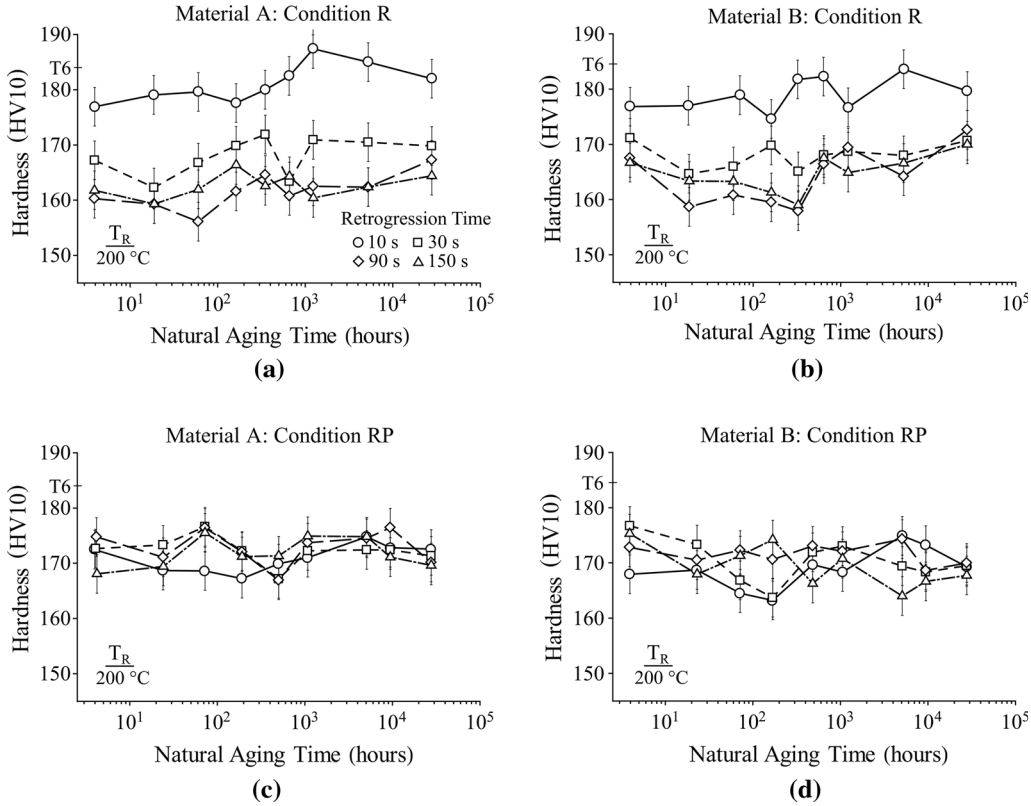


Fig. 7—Vickers hardness (HV10) measurements after retrogression at 200 °C for 10, 30, 90, and 150 s are presented as functions of natural aging time on logarithmic scales for (*a*) material A and (*b*) material B. Hardness measurements after retrogression at 200 °C for 10, 30, 90, and 150 s, natural aging at 21 °C for 1 week, and simulated paint baking at 180 °C for 30 min are shown as functions of natural aging time for (*c*) material A and (*d*) material B. Initial hardnesses in the as-received T6 condition, measured as 183.8 HV10 for material A and 184.8 HV10 for material B, are noted.

Figure 3. Only data from tensile tests on material A are presented in this study; the behaviors observed for material B are not appreciably different from those of material A. Figure 8 presents plots of true stress against true strain for tests conducted on material A at 200 °C. Data from specimens with the rolling direction oriented parallel and perpendicular to the tensile direction are presented in Figures 8(a) and (b), respectively. Neither flow stress nor rupture strain varied markedly with strain rate or the orientation of the rolling direction relative to the tensile direction. Flow stress remained between 364 and 396 MPa for all tests, and rupture, defined as the complete failure of the specimen into two distinct pieces, occurred at an average true strain of 0.2 and did not vary by more than 0.03 between the three strain rates tested. Failure was by flow localization, *i.e.*, necking, quickly followed by rupture. The downward trend in flow stress near rupture is an artifact from the calculation of true stress that results from necking behavior; local geometry in the necked region could not be measured during the test. The benefit of presenting these data as true values is in demonstrating the absence of any significant strain hardening prior to neck development.

Tensile data from the present study are presented in Figure 9 on a plot of true stress against true strain for material A at temperatures of 21 °C, 200 °C, and 300 °C. Data from Wang *et al.*[16] and Sotirov *et al.*[17] for AA7075-T6 tested at temperatures from 180 °C up to 260 °C are also shown in Figure 9. These data together demonstrate the tensile ductilities possible from AA7075-T6 at temperatures up to 300 °C for strain rates between $5\times10^{-2}$ and 1 $s^{-1}$. Table VI summarizes the results from tensile tests conducted in this study. Elongation-to-rupture ($e_r$ (pct) in Table VI) in material A at 200 °C, a temperature suitable for retrogression, is double that achieved at room temperature. Data from the literature likewise demonstrate that ductility in AA7075-T6 is increased by a factor of 2, approximately, at temperatures of 180 °C to 230 °C. It is noteworthy that increasing temperature from 230 °C up to 300 °C does not significantly improve tensile ductility. Even when comparing data from within one set of tests, the ductility at 300 °C is only slightly greater than that at 200 °C, for a strain rate of $5 \times 10^{-2}$ $s^{-1}$.

Tensile behavior of material A between 460 °C and 520 °C is summarized in Figure 10 and Table VI. Ductility between 460 °C and 520 °C is much greater than that at 200 °C. Flow stress data at a true strain of 0.1 are presented in Figure 10 as a plot of the logarithm of true-strain rate against the logarithm of true stress normalized by the dynamic, unrelaxed, temperature-dependent elastic modulus, *i.e.*, $\sigma/E$. Elastic modulus data from Köster for aluminum were used for the stress normalization.[52] The stress exponent of 5, measured from the slope of the data in Figure 10, is that expected of dislocation-climb-controlled creep deformation.[53] Data from different temperatures, taken at constant values of $\sigma/E$, were used to calculate the activation energy for creep using the following relationship,[53]

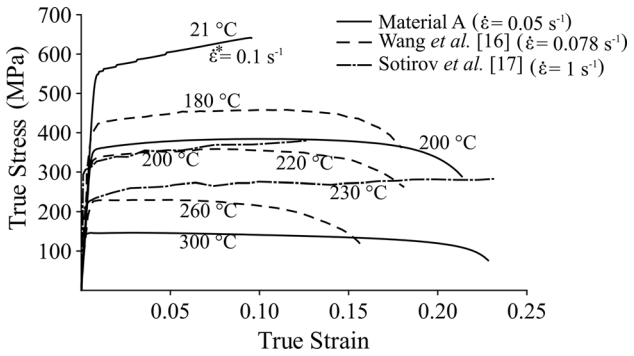


Fig. 9—True-stress and true-strain data from uniaxial tensile tests of material A are presented with tensile data from Wang *et al.*[16] and Sotirov *et al.*[17] for comparison. The data from this study and the literature were acquired from uniaxial tensile tests conducted at the temperatures and approximately constant true-strain rates provided. *Initial strain rate is reported for the test of material A at 21 °C because constant true-strain rate was not maintained through the duration of this test. Specimens were oriented with the RD parallel to the TD for tests completed in this study on material A and tests completed by Wang *et al.*[16] The orientation of the RD with respect to the TD was not reported by Sotirov *et al.*[17]

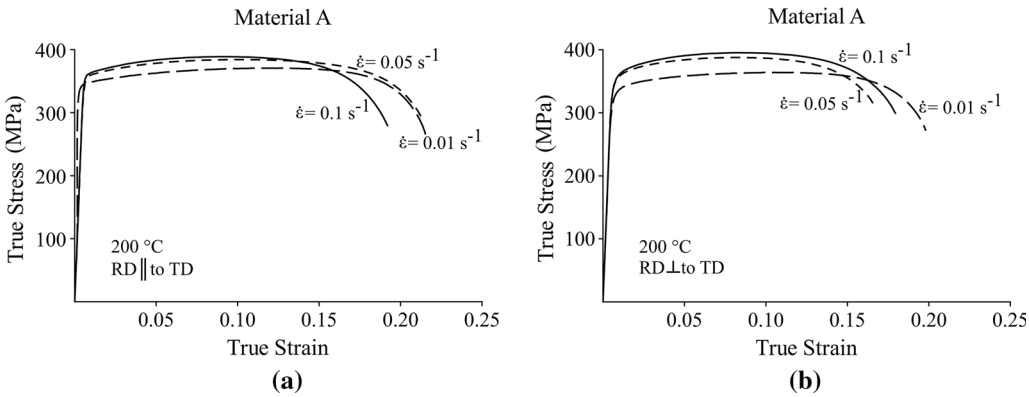


Fig. 8—True-stress and true-strain data from uniaxial tensile tests of material A at 200 °C with rapid heating. Testing was conducted at approximately constant true-strain rates of 0.1, 0.05, and 0.01 $s^{-1}$. Specimens were oriented with (*a*) the RD parallel to the TD and (*b*) the RD perpendicular to the TD.

**Table VI. The Results of Uniaxial Tensile Tests on Material A According to Test Temperature ($T$), Material Temper/Condition Prior to Testing, Tensile Axis Orientation, and True-Strain Rate ($\dot{\varepsilon}$)**

| $T$ (°C) | Temper | Orientation | $\dot{\varepsilon}$ ($s^{-1}$) | $e_r$ (Pct) | RA (Pct) | $\sigma_{max}$ (MPa) |
|---|---|---|---|---|---|---|
| 21 | T6 | RD \|\| TD | 0.1* | 10.0 | 20.0 | 641 |
| | sol. | RD \|\| TD | 0.1* | 16.0 | 23.5 | 601 |
| 200 | T6 | RD \|\| TD | 0.01 | 24.2 | 38.0 | 371 |
| | | | 0.05 | 24.0 | 35.7 | 385 |
| | | | 0.1 | 21.5 | 37.3 | 389 |
| | | RD ⊥ TD | 0.01 | 22.0 | 39.6 | 364 |
| | | | 0.05 | 18.3 | 33.7 | 388 |
| | | | 0.1 | 19.9 | 36.1 | 396 |
| 300 | sol. | RD \|\| TD | 0.05 | 25.6 | 72.9 | 146 |
| 460 | sol. | RD \|\| TD | 0.0048 | 109 | 74.5 | 26.2 |
| | | | 0.005 | 107 | 70.7 | 26.2 |
| | | | 0.006 | 106 | 70.4 | 27.3 |
| | | | 0.01 | 113 | 74.2 | 30.1 |
| 480 | sol. | RD \|\| TD | 0.0003 | 125 | 53.0 | 11.6 |
| | | | 0.001 | 75.2 | 43.6 | 15.7 |
| | | | 0.003 | 63.5 | 50.6 | 19.9 |
| | | | 0.01 | 74.6 | 67.3 | 26.0 |
| | | | 0.01 | 105 | 52.0 | 25.3 |
| | | | 0.03 | 111 | 67.4 | 31.4 |
| | | | 0.1 | 94.0 | 64.3 | 39.2 |
| | | | 0.3 | 105 | 60.8 | 48.7 |
| 500 | sol. | RD \|\| TD | 0.0177 | 79.6 | 53.3 | 24.1 |
| | | | 0.02 | 71.4 | 53.4 | 24.8 |
| | | | 0.02 | 74.9 | 52.0 | 24.8 |
| | | | 0.052 | 65.4 | 49.6 | 29.8 |
| 520 | sol. | RD \|\| TD | 0.035 | 25.2 | 30.9 | 22.5 |
| | | | 0.04 | 20.2 | 29.9 | 23.2 |
| | | | 0.088 | 25.5 | 24.9 | 27.2 |

Results are reported for tensile elongation-to-rupture ($e_r$), reduction-in-area at rupture (RA), and maximum true flow stress ($\sigma_{max}$). (RD is rolling direction. TD is tensile direction.).

*Initial strain rate is reported.

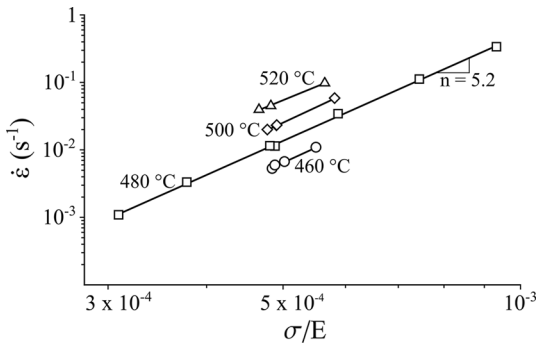


Fig. 10—The logarithm of true-strain rate is plotted against the logarithm of true stress normalized by the dynamic, unrelaxed, temperature-dependent elastic modulus for uniaxial tensile tests conducted on material A from 460 °C to 520 °C. Data are shown for a true-strain value of 0.1. Specimens were oriented with the RD parallel to the TD.

$$Q_C = -R\frac{\partial \ln \dot{\varepsilon}}{\partial 1/T}\bigg|_{\sigma/E}, \qquad [2]$$

where $Q_C$ is the activation energy for creep deformation; $R$ is the universal gas constant; $\dot{\varepsilon}$ is the true-strain rate; and $T$ is absolute temperature. The activation energy for creep, is calculated to be within the range of 166 to 170 kJ/mol. for $\sigma/E$ values of $4.9 \times 10^{-4}$, $5.2 \times 10^{-4}$, and $5.5 \times 10^{-4}$.

## IV. DISCUSSION

### A. *Retrogression*

The retrogression behaviors of materials A and B, as presented in Figure 3, can be grouped into two categories based on whether hardness is (1) recoverable or (2) unrecoverable by reaging after retrogression. Among retrogression treatments conducted at 200 °C, 225 °C, and 250 °C, each demonstrates a local minimum in hardness and hardness lost during retrogression is 80 to 100 pct recoverable from the vicinity of these local minima by the standard reaging treatment (24 hours at 120 °C). This is illustrated by comparing hardness after retrogression in Figure 3 to hardness after reaging with the simulated paint bake in Figure 5 and by comparing the RA and RP curves to the R curves in Figures 6(a) through (d). Data in the literature demonstrate through TEM and SAED that retrogression at these temperatures either partially dissolves the fine (5 to 10 nm) $\eta'$ and $\eta$ precipitates characteristic of peak-aged AA7075-T6 or transforms and coarsens these into larger (> 20 nm) $\eta$ precipitates, particularly at grain boundaries.[31–36]

Because the recovery of hardness by reaging is possible among the conditions studied here only after retrogression temperatures less than or equal to 250 °C for times limited by the temperature-dependent values of $t_r^{max}$, the mechanism of reaging likely depends on limiting species diffusion during retrogression. It is likely necessary to limit the diffusion distances of Zn and/or Mg out of and away from $\eta'$ and $\eta$ precipitates during their dissolution and limit diffusion of Zn and/or Mg into larger $\eta$ precipitates during coarsening. Retaining high local concentrations of Zn and/or Mg near partially dissolved precipitates will support the reformation of these precipitates during reaging. If full dissolution of a precipitate occurs, a high local concentration of Zn and/or Mg can accelerate nucleation and growth of a new precipitate at the same location. As retrogression time and temperature increase, the increased homogenization of these species because of diffusion within the Al lattice and the possibility of tying up solute elements in significantly coarsened precipitates is likely to prevent effective reaging, and hardness is then unrecoverable in the practical sense. Retrogression at temperatures of 300 °C and higher does not demonstrate a local hardness minimum within the scope of experimental data shown in Figure 3, as any local minimum in hardness occurs at times too short to be readily measured. At these retrogression temperatures, complete dissolution of fine $\eta'$ and $\eta$ precipitates and a fairly homogeneous distribution of the atomic species Mg and Zn likely occur after relatively short times. Large $\eta$ precipitates and even larger alternative precipitation products, such as the T-phase ($(AlZn)_{49}Mg_{32}$), are then likely.[34,42] Consequently, strength cannot be recovered after such retrogression treatments by simple reaging because solute elements are consumed by the large precipitation products preventing the formation of fine $\eta'$ and $\eta$ precipitates. A full solutionizing treatment and the usual artificial aging practice would be required after retrogression at temperatures of 300 °C and higher.

Figures 3 and 6 demonstrate that material A exhibits a larger drop in hardness than material B under identical retrogression conditions by approximately 3 to 5 pct in hardness loss. The reason for this was not explored in this study, but it is likely a result of composition differences between these materials. Table II demonstrates that material B contains more Zn, Mg, Si, and Cu than material A. These differences are expected to affect retrogression behavior, but further investigation is needed to confirm this expectation. Regardless, controlling composition is necessary to achieve predictable retrogression behavior and possibly adjust it for a desired performance.

Figure 4 proposes the use of temperature-compensated time, $\tau$, as defined by Eq. [1] to predict retrogression times that produce a local hardness minimum after retrogression at given retrogression temperatures. In this case, the local hardness minimum occurs at an approximately constant value of $3.6 \times 10^{-9}$ seconds for temperature-compensated time, $\tau_r^*$, across a range of retrogression temperatures. The activation energy used in calculating this reduced time for Figure 4 is 95 kJ/mol, which is that determined in a previous study[37] for precipitate dissolution in similar alloys at temperatures similar to those used for retrogression in this study. It is hypothesized that this value can be interpreted as approximately the activation energy for Zn diffusion in Al, as in the previous investigation,[37] because the rate of Zn diffusion is faster than Mg in Al.[47–51] The rapidity of $\eta'$ and $\eta$ precipitate dissolution, from the perspective of strength loss, is likely controlled by the fastest diffusing species among those which comprise these precipitates, Zn in this case. The activation energy for the diffusion of Zn in Al, Al-Zn-Mg, and Al-Zn-Cu materials obtained from traditional tracer diffusion methods is reported in the literature as approximately 120 kJ/mol,[47–51] but these data are for higher temperatures than those used for retrogression. The extant literature on diffusion provides data only for the diffusion of Mg and Zn in Al at temperatures higher than those used for recoverable retrogression (200 °C to 250 °C) in this study,[47–51] which leaves a need for additional diffusion data to test the interpretation proposed here. The value for activation energy could also be determined empirically by forcing the data in Figure 4 to collapse onto a single curve. Regardless of these details, Eq. [1] provides a tool of practical utility for predicting appropriate retrogression times and temperatures for a potential retrogression-forming process using AA7075-T6.

### B. *Reaging*

Reaging AA7075 after a retrogression treatment is necessary to recover strength lost during that treatment and is ideally performed for 24 hours at 120 °C, the standard artificial aging temperature for AA7075.[19] Figure 6 demonstrates that peak-aged (T6) hardness was fully recovered (within 5 pct of the measured T6 value) in materials A and B after retrogression at 200 °C and 225 °C by reaging at 120 °C for 24 hours, if retrogression time did not pass $t_r^{max}$, as shown in Figure 1(a). For materials A and B, $t_r^{max}$ is likely beyond 150 seconds for retrogression at 200 °C and is between 30 and 90 seconds for retrogression at 225 °C (see Figure 6). The literature indicates that this reaging procedure produces a microstructure containing numerous fine $\eta'$ precipitates and some $\eta$ precipitates distributed throughout the aluminum matrix, from which peak-aged strength is derived. Park and Ardell demonstrated that the numbers of $\eta'$ and $\eta$ precipitates present in retrogressed-and-reaged (RRA) AA7075 and in AA7075-T6 are approximately equal.[34]

Reaging was also performed with a simulated paint-bake cycle of 180 °C for 30 minutes. If strength lost during retrogression forming is recovered through the paint bake, no additional heat treatments or changes to current paint-baking practices would be required to provide nearly peak-aged strength in final components. Figure 6 demonstrates that hardness after retrogression at 200 °C and 225 °C for times near $t_r^*$ was recovered to within 5 to 10 pct of the peak-aged value by reaging

with the simulated paint bake. The simulated paint-bake temperature of 180 °C, which reflects one current industry practice, exceeds the temperatures recommended for standard peak-aging (120 °C for 24 hours) and the second step of standard over-aging (163 °C for 27 hours) treatments.[19,42] Reaging with the simulated paint bake likely produces fewer fine $\eta'$ and $\eta$ precipitates compared to reaging at 120 °C for 24 hours, and the average precipitate size is thereby expected to be larger. However, hardness after reaging with the simulated paint bake is typically greater than that of over-aged AA7075-T7, nominally 155 HV10.[19] We surmise, based upon characterization of AA7075 microstructures in the peak-aged, over-aged, and retrogressed conditions presented in the literature,[31–36] that the short duration of the simulated paint bake avoids over-aging while still producing fine precipitate reformation. The short duration of the simulated paint bake may largely avoid (1) the coarsening of large $\eta$ precipitates, (2) the transformation of $\eta'$ to $\eta$, and (3) the further dissolution of fine $\eta'$ and $\eta$ precipitates. Further characterization of the microstructures produced would be necessary to more fully understand these effects.

A two-step reaging procedure after retrogression (RAP—see Table IV) was also investigated for materials A and B. For the two-step procedure, the material was first retrogressed at 200 °C or 225 °C, reaged at 120 °C for 24 hours, and then subjected to the simulated paint bake. This two-step procedure suggests one possible manufacturing route in which material is subjected to a standard reaging treatment following retrogression forming and is subsequently processed through a paint-bake cycle. As demonstrated by the data in Figure 6, the RAP process provides no substantive advantage in final hardness, and through inference, final peak strength, over applying only a simulated paint bake after retrogression (RP—see Table IV). The RAP process generally produces slightly less hardness recovery than does the RP process alone. These data suggest that a standard reaging treatment following retrogression, or retrogression forming, should be avoided if a paint bake is to follow.

After retrogression at 225 °C, the simulated paint bake restored significant hardness in material A but not in material B, as illustrated by Figures 6(c) and (d). Figures 6(a) and (b) illustrate that a standard reaging treatment after retrogression at 200 °C in material A recovers approximately 3 pct more hardness than for material B. These differences in reaging behavior can likely be attributed to compositional differences between the materials.

The conditions appropriate to perform retrogression concurrently with warm-forming and to recover nearly peak-aged strength after a simulated paint bake were determined. Hardness can be recovered to within 5 to 10 pct of the peak-aged (T6) condition in both materials A and B by a simulated paint bake following retrogression treatments conducted at 200 °C for up to 150 seconds. This offers a reasonable window for simultaneous warm forming at 200 °C, which is necessary to enable a practical retrogression-forming technology. While not addressed in this study, the effect of strain on RRA behavior in AA7075 sheet material should be explored prior to the implementation of RRA-forming.

### C. *Tensile Tests*

Tensile elongation and reduction-in-area at rupture are two of the many measures useful for characterizing sheet material formability. Figure 11(a) presents tensile elongation and reduction-in-area at rupture for material A as a function of test temperature. These data are from uniaxial tensile tests conducted at temperatures from 21 °C to 520 °C. Large differences between tensile elongation and reduction-in-area measurements at a given temperature suggest significant flow localization, *i.e.*, necking, prior to rupture. Maximum true flow stress is presented in Figure 11(b) as a function of test temperature; this value represents a nearly steady-state flow stress for tests at 200 °C and higher temperatures, as is evident from Figures 8 and 9. Figure 12 displays specimens before and after uniaxial tensile tests conducted on material A at 21 °C, 200 °C, 300 °C, 460 °C,

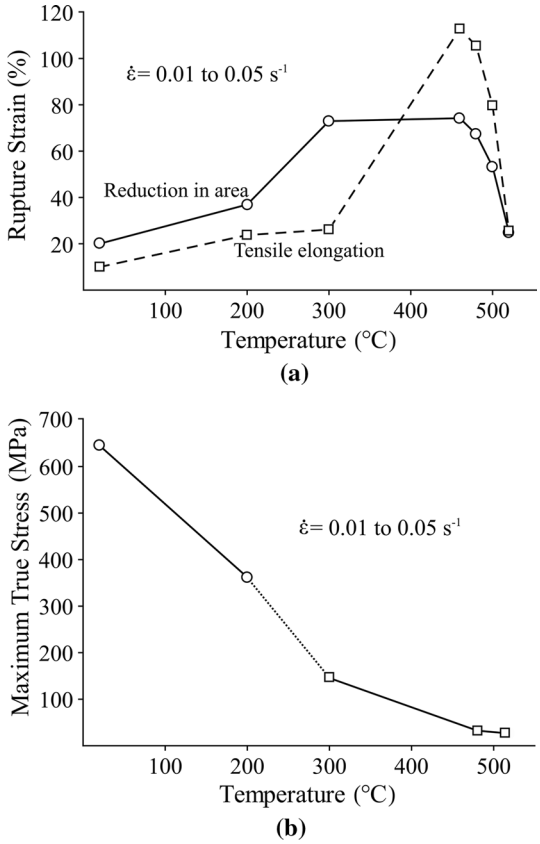


Fig. 11—(*a*) Tensile elongation and reduction-in-area at rupture are plotted as a function of test temperature for material A. (*b*) Maximum true flow stress is plotted against test temperature for material A. Tests at room temperature and 200 °C were on material A in the T6 temper; all other tests were conducted on material A in the solutionized condition. The data reported were acquired from uniaxial tensile tests at true-strain rates, $\dot{\varepsilon}$, between 0.01 and 0.05 $s^{-1}$. Specimens were oriented with the RD parallel to the TD.

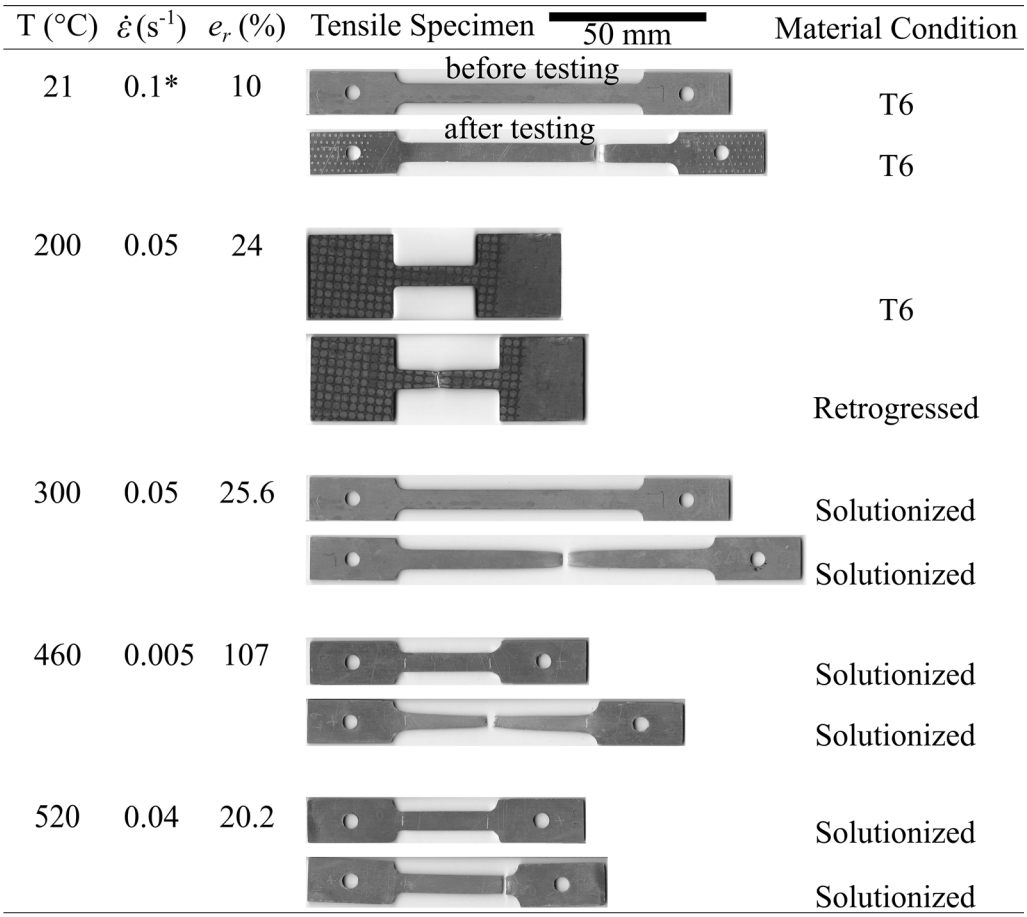


* Initial strain rate is reported.

Fig. 12—Tensile specimens before and after testing in uniaxial tension according to test temperature ($T$) and true-strain rate ($\dot{\varepsilon}$). Specimens were oriented with the RD parallel to the TD.

and 520 °C. Data from these tests are summarized in Table VI.

The tensile elongation of AA7075-T6, as represented by material A, at room temperature is limited to approximately 10 pct (see Figure 9). Modest flow localization is evident for this specimen in Figure 12 and from the discrepancy between reduction-in-area and tensile elongation at rupture in Figure 11(a). Figure 11(b) demonstrates a maximum true flow stress of 641 MPa at room temperature. This high strength is useful in service but makes room-temperature forming challenging because it produces very high stamping forces and significant spring back. These issues and limited ductility at room temperature severely restrict the complexity of shapes that can be stamped from AA7075-T6 at room temperature. Tensile elongation at room temperature is improved to 17 pct when the material is in the O temper, the softest condition for AA7075.[19] However, the O temper introduces significant problems with temper stability during storage and requires aging at 120 °C for 24 hours after forming to achieve the T6 temper, adding additional complexity and cost to the manufacturing process.

Data from the warm tensile tests, defined as temperatures near 200 °C in this study, suggest significant improvements in ductility and reductions in strength that benefit the retrogression-forming process. Figure 11(a) demonstrates that the ductility of AA7075-T6 is improved twofold, to 20 pct tensile elongation, at 200 °C compared to room temperature. Modest necking is suggested in Figure 12 and from the discrepancy between reduction-in-area and tensile elongation at rupture, shown in Figure 11(a). This degree of necking is similar to that observed at room temperature. The peak true flow stress is reduced from 641 MPa at room temperature to approximately 380 MPa at 200 °C. This flow stress at 200 °C is 40 pct less than that of AA7075-T6 at room temperature, significantly less than that for over-aged AA7075-T7 at room temperature ($\approx$ 500 MPa), and only 130 MPa greater than that for AA7075-O at room temperature ($\approx$ 250 MPa).[19] The specific mechanism responsible for this reduction in flow stress at warm temperatures was not determined during this study, but it is expected to be related to the effects that produce retrogression at these temperatures. Regardless of the active mechanisms, these data indicate

that warm temperatures near 200 °C significantly increase the tensile ductility of AA7075-T6 sheet material. The hardness data acquired confirm that strength lost during warm forming can be recovered if warm forming is conducted within the times specified for recoverable retrogression. This study demonstrates that nearly peak-aged strength (within 5 to 10 pct) can be recovered through the paint bake after warm forming.

Tensile ductility at 300 °C is not significantly improved compared to that at 200 °C. Necking at 300 °C is more severe than at 200 °C, as is demonstrated in Figure 12. Furthermore, strength cannot be effectively recovered through the simulated paint bake after retrogression at temperatures greater than 225 °C. Consequently, forming at temperatures between 225 °C and 300 °C is unlikely to be of practical use for sheet forming applications.

Tensile tests at 460 °C and 480 °C provided the greatest tensile ductilities, from 63.5 up to 125 pct. Failure at these high temperatures occurred by cavitation after significant necking, in contrast to the necking-controlled failures observed at lower temperatures. Note from Figure 11(a) that tensile ductility decreases significantly as temperature rises above 480 °C. This is because of a rapid onset in cavitation prior to significant necking above 480 °C. At 520 °C, tensile ductility is comparable to that at 200 °C. The onset of cavitation failure at temperatures above 460 °C for strain rates greater than $10^{-3}$ $s^{-1}$ is in agreement with similar data reported in the literature.[20,54] Forming at temperatures between 460 °C and 480 °C might be useful in applications where high formability is desired, the initial AA7075 temper is of no concern and subsequent heat treatments to achieve peak-aged (T6) strength that are not subject to time limits are acceptable. Hot-forming practice may be useful for low-volume production parts, but for high-volume production parts, such as in the automotive industry, high-temperature forming is cost-challenged and retrogression forming may provide a better alternative.

## V. CONCLUSIONS

The retrogression-reaging behaviors and tensile plasticity responses of two commercial AA7075-T6 sheet materials were experimentally evaluated across a range of temperatures. The following conclusions are derived from these new data.

1. For both AA7075-T6 materials considered in this study, retrogression at 200 °C for 150 seconds or less produces a loss in hardness that is recoverable to within 5 to 10 pct of the original peak (T6) strength by reaging with a simulated paint bake at 180 °C for 30 minutes. The corresponding tensile ductility of AA7075-T6 at 200 °C is 20 pct, double that at room temperature.
2. The peak-flow stress of AA7075-T6 at 200 °C is 40 pct less than that at room temperature, *e.g.*, 396 *vs.* 640 MPa. This result suggests that the press forces required for retrogression forming are significantly less than those required for room-temperature stamping.
3. The two-step process of reaging at 120 °C for 24 hours prior to a paint bake following retrogression at 200 °C is less effective at restoring hardness than applying the simulated paint bake alone after retrogression.
4. Retrogression times and temperatures appropriate for recovering hardness by reaging are predicted accurately across several temperatures by the temperature-compensated time, $\tau = t \cdot e^{-Q/RT_R}$, where t and $T_R$ are the retrogression time and temperature, respectively, and $Q$ is the relevant activation energy. This activation energy, taken as 95 kJ/mol,[37] is thought to reflect the lattice diffusion of Zn atoms in Al in the vicinity of $\eta$ and $\eta$' precipitates during their dissolution.
5. AA7075 alloying effects are important to retrogression and reaging behavior as material A more readily recovered hardness through reaging after retrogression than did material B. This effect is particularly noticeable after retrogression at temperatures of 225 °C and above.
6. Tensile ductility in the AA7075-T6 materials studied does not substantially increase at temperatures up to 300 °C compared to at 200 °C. Tensile ductility peaks between 460 °C to 480 °C, but hardness cannot be recovered to peak (T6) strength by a simple paint-bake reaging process after deformation at temperatures greater than 300 °C.


## ACKNOWLEDGMENTS

This work was supported by the National Science Foundation under Grant Number CMMI-1634495 and by General Motors.


## DATA AVAILABILITY

The raw/processed data required to reproduce these findings cannot be shared at this time as the data also form part of an ongoing study.



## REFERENCES


1. M. Kahl (ed.): Special Report: Vehicle Lightweighting, Automotive World Ltd., 2016. https://www.automotiveworld.com/research/special-report-vehicle-lightweighting. Accessed December 2017.

2. General Motors 2017 Sustainability Report. https://www.gmsustainability.com/_pdf/downloads/GM_2017_SR.pdf. Accessed August 2018.
3. G.J. Huebner Jr. and D.J. Gasser: *SAE Tech. Pap. Ser.,* 1973, no. 730518.
4. D.G. Adams, J.A. DiCello, C. Hoppe, A.S. Kasper, A.N. Keisoglou, and W.W. McVinnie: *SAE Tech. Pap. Ser.,* 1975, no. 750221.
5. M. Pfestorf and J. van Rensburg: *SAE Tech. Pap. Ser.,* 2006, no. 2006-01-1405.
6. M. Verbrugge, T. Lee, P. Krajewski, A. Sachdev, C. Bjelkengren, R. Roth, and R. Kirchain: *Mater. Sci. Forum*, 2009, vol. 618, pp. 411–18.
7. H. Kim, G.A. Keoleian, and S.J. Skerlos: *J. Ind. Ecol.*, 2011, vol. 15, pp. 64–80.
8. A.I. Taub, P.E. Krawjewski, A.A. Luo, and J.N. Owens: *JOM*, 2007, vol. 59, pp. 48–57.
9. G.S. Cole and A.M. Sherman: *Mater. Charact.*, 1995, vol. 35, pp. 3–9.
10. X. Fan, Z. He, W. Zhou, and S. Yuan: *J. Mater. Process. Technol.*, 2016, vol. 228, pp. 179–85.
11. X. Fan, Z. He, S. Yuan, and K. Zheng: *Mater. Sci. Eng. A*, 2013, vol. 573, pp. 154–60.
12. AMAG Austria Metall AG AluReport03.2014. https://www.amag-al4u.com/fileadmin/user_upload/amag/Downloads/AluReport/EN/AR-2014-3-EN-S14-15-.pdf. Accessed December 2017.
13. N.R. Harrison and S.G. Luckey: *SAE Int. J. Mater. Manuf.*, 2014, vol. 7, pp. 567–73.
14. A.A. Luo: *JOM*, 2002, vol. 54, pp. 42–48.
15. ASM International: *ASM Handbook Volume 2, Properties and Selection: Nonferrous Alloys and Special-Purpose Materials*, 10th ed., ASM International, Materials Park, 1990, pp. 29–61.
16. H. Wang, Y. Luo, P. Friedman, M. Chen, and L. Gao: *Trans. Nonferrous Metals Soc. China*, 2012, vol. 22, pp. 1–7.
17. N. Sotirov, P. Simon, C. Chimani, D. Uffelmann, and C. Mezler: *Key Eng. Mater.*, 2012, vol. 504, pp. 955–60.
18. M. Zhou, Y.C. Lin, J. Deng, and Y. Jiang: *Mater. Des.*, 2014, vol. 59, pp. 141–50.
19. J.R. Davis (ed.): *ASM Specialty Handbook: Aluminum and Aluminum Alloys*, ASM International, Materials Park, 1993, pp. 72-73.
20. E.M. Taleff, P.J. Nevland, and P.E. Krajewski: *Metall. Mater. Trans. A*, 2001, vol. 32A, pp. 1119–30.
21. P.F. Bariani, S. Bruschi, A. Ghiotti, and F. Michieletto: *CIRP Ann-Manuf. Technol.*, 2013, vol. 62, pp. 251–54.
22. F. Ozturk, A. Sisman, S. Toros, S. Kilic, and R.C. Picu: *Mater. Des.*, 2010, vol. 31, pp. 972–75.
23. D. Daniel, J.L. Hoffmann, G. Plassart, and J. Prunier: *SAE Tech. Pap. Ser.*, 2002, no. 2002-01-2012.
24. S.J. Murtha: *SAE Tech. Pap. Ser.*, 1995, no. 950718.
25. R.G. Davies: *Metall. Mater. Trans. A*, 1979, vol. 10A, pp. 113–18.
26. M.S. Rashid: *Annu. Rev. Mater. Sci.*, 1981, vol. 11, pp. 245–66.
27. J.H. Bucher and E.G. Hamburg: *SAE Tech. Pap. Ser.*, 1977, no. 770164.
28. J.K. Park and A.J. Ardell: *Metall. Trans. A*, 1983, vol. 14, pp. 1957–65.
29. J.T. Carter: General Motors Corp., Warren, MI, private communication, 2017.
30. B.M. Cina: U.S. Patent 3,856,584, 1974.
31. J.K. Park: *Mater. Sci. Eng. A*, 1988, vol. 103, pp. 223–31.
32. M. Kanno, I. Araki, and Q. Cui: *Mater. Sci. Technol.*, 1994, vol. 10, pp. 599–603.
33. K. Rajan, W. Wallace, and J.C. Beddoes: *J. Mater. Sci.*, 1982, vol. 17, pp. 2817–24.
34. J.K. Park and A.J. Ardell: *Metall. Mater. Trans. A*, 1984, vol. 15A, pp. 1531–43.
35. N.C. Danh, K. Rajan, and W. Wallace: *Metall. Mater. Trans. A*, 1983, vol. 14A, pp. 1843–50.
36. F. Viana, A.M.P. Pinto, H.M.C. Santos, and A.B. Lopes: *J. Mater. Process. Technol.*, 1999, vol. 92, pp. 54–59.
37. D.C. Balderach, J.A. Hamilton, E. Leung, M.C. Tejeda, J. Qiao, and E.M. Taleff: *Mater. Sci. Eng. A*, 2003, vol. 339, pp. 194–204.
38. Registration Record Series Teal Sheets: International Alloy Designations and Chemical Composition Limits for Wrought Aluminum and Wrought Aluminum Alloys: *The Aluminum Association*, January 2015, p. 12.
39. Alcoa Mill Products: *Alloy 7075 Plate and Sheet*. http://www.calm-aluminium.com.au/Documents/alloy7075techsheet.pdf. Accessed December 2017.
40. L.J. Barker: *Trans. Am. Soc. Metals*, 1950, vol. 42, pp. 347–56.
41. ASTM Standard E112-13: *ASTM International*, 2013.
42. G.E. Totten (ed.): *ASM Handbook Volume 4E: Heat Treating of Nonferrous Alloys*, ASM International, Materials Park, 2016, pp. 214–95.
43. ASTM Standard E8/E8M-16a: *ASTM International*, Materials Park, 2016.
44. ASTM Standard E21-09: *ASTM International*, Materials Park, 2009.
45. ASTM Standard E2448-11e1: *ASTM International*, Materials Park, 2011.
46. S. Arrhenius: *Z. Phys. Chem. (Leipzig)*, 1889, vol. 4, pp. 96–116.
47. J.E. Hilliard, B.L. Averbach, and M. Cohen: *Acta. Metall.*, 1959, vol. 7, pp. 86–92.
48. N.L. Peterson and S.J. Rothman: *Phys. Rev. B*, 1970, vol. 1, pp. 3264–73.
49. S. Fujikawa and K. Hirano: *Trans. Jpn. Inst. Metals*, 1976, vol. 17, pp. 809–18.
50. K. Hirano and S. Fujikawa: *J. Nucl. Mater.*, 1978, vol. 69, pp. 564–66.
51. DL Beke, I Gödény, and FJ Kedves: *Philos. Mag. A*, 1983, vol. 47, pp. 281–99.
52. W. Koster: *Z. Metallkd.*, 1948, vol. 39, pp. 1–12.
53. O.D. Sherby and P.M. Burke: *Prog. Mater. Sci.*, 1968, vol. 13, pp. 323–90.
54. D.A. Miller and T.G. Langdon: *Trans. Jpn. Inst. Metals*, 1980, vol. 21, pp. 123–25.